High order numerical methods for the space non-homogeneous Boltzmann equation

Francis Filbet [a], Giovanni Russo [b,*]

[a] *IRMA – Université Louis Pasteur, 7 rue René Descartes, 67084 Strasbourg, France*
[b] *Università di Catania, Viale Andrea Doria 6, 95125 Catania, Italy*

Abstract

In this paper we present accurate methods for the numerical solution of the Boltzmann equation of rarefied gas. The methods are based on a time splitting technique. The transport is solved by a third order accurate (in space) positive and flux conservative (PFC) method. The collision step is treated by a Fourier approximation of the collision integral, which guarantees spectral accuracy in velocity, coupled with several high order integrators in time. Strang splitting is used to achieve second order accuracy in space and time. Several numerical tests illustrate the properties of the methods.
© 2003 Elsevier Science B.V. All rights reserved.

Keywords: Boltzmann equation; Rarefied gas dynamics; Spectral methods; Splitting algorithms

1. Introduction

In a microscopic description of rarefied neutral gas, the gas particles move by a constant velocity until they undergo binary collisions. In a kinetic picture, the properties of the gas are described by a density function in phase space, $f(t, x, v)$, called the *distribution function*, which gives the number of particles per unit volume in phase space at time t. The distribution function satisfies the Boltzmann equation, an integro-differential equation, which describes the effect of the free flow and binary collisions between the particles.

The numerical solution of the Boltzmann equation represents a real challenge for numerical methods. This is essentially due to the nonlinearity, to the large number of variables (t for the time, two 3D vectors x for space and v for velocity) and to the fivefold integral that defines the collision operator. Furthermore, this integration has to be handled carefully since it is at the basis of the macroscopic properties of the Boltzmann equation.

Among the different approaches for the approximation of the Boltzmann equation, we may distinguish between deterministic and Monte-Carlo methods. The first usually provide accurate oscillations-free

solutions, but they are much more expensive than Monte-Carlo methods with the same number of discrete degrees of freedom. For example, if we denote by n the number of parameters which characterize the density with respect to the velocity variables in a space homogeneous calculation, the computational cost of a conventional deterministic method for the evaluation of the collisional integral is much larger than n^2. As a consequence most numerical computations are based on probabilistic Monte-Carlo techniques at different levels. Examples are the *direct simulation Monte-Carlo method* (DSMC) by Bird [2] and the modified Monte Carlo method by Babovsky and Nanbu [1,13]. For a detailed description of such methods we refer to [2,6].

Probabilistic particle methods present different advantages. First, the computational cost for advancing by a typical collision time Δt is strongly reduced and approximately can be considered of the order of the number of points n. Second, these methods do not need any artificial boundary in the velocity space. In fact, particles can have any velocity and thus the discretization points are always well defined independently of the physical problem. Finally, particle methods make a much more efficient use of computer memory, since the particles concentrate where the function is not small, and memory is not wasted representing a function which is virtually zero in most phase space. For this reason, particle methods have no competitor for situations very far from thermodynamical equilibrium.

At variance, in addition to the computational complexity, a major problem associated with deterministic methods that use a fixed discretization in the velocity domain is that the velocity space is approximated by a finite region. Hence, a large region with a huge number of discretization points is required in problems with very high Mach numbers, which greatly increase the computing effort. In spite of these difficulties, deterministic methods can be much more accurate, and can be competitive with Monte-Carlo methods for problems in which the solution is not very far from thermodynamical equilibrium, and high accuracy is required. In the framework of deterministic approximations, the most popular class of methods is based on the so called *discrete velocity models* (DVM) of the Boltzmann equation. All these methods [4,10,11,20] make use of regular discretizations on hypercubes in the velocity field and construct a discrete collision mechanics on the nodes of the hypercube in order to preserve the main physical properties. Although the numerical results have shown that these schemes are able to avoid fluctuations, their computational cost is high (in general $O(n_a n^2)$, where n_a is the number of parameters used for the angular integration, typically in such methods $n_a \approx O(n^{1/3})$) and, due to the particular choice of the integration points imposed by the conservation properties, the order of accuracy is lower than that of a standard quadrature formula applied directly to the collision operator. Hence we observe that the requirement of maintaining at a discrete level the main physical properties of the continuous equation makes it extremely difficult to obtain high order accuracy. On the other hand, even if conservation properties are not imposed from the beginning, an accurate scheme would provide an accurate approximation of the conserved quantities.

In [16], Pareschi and Perthame developed a discretization of the collision operator based on expanding in Fourier series the distribution function with respect to the velocity variable. The resulting spectral approximation can be evaluated with a computational cost of $O(n^2)$ which is lower than that of previous deterministic methods. Bobylev and Rjasanow [3] used a Fourier transform approximation of the distribution function, and they were able to obtain exact conservation by a suitable modification of the evolution equations for the Fourier coefficients. In [18], Pareschi and Russo developed a scheme based on the approximation of the distribution function by a periodic function in phase space, and by its discretization by Fourier series. Evolution equations for the Fourier modes are explicitly derived for the variable hard sphere (VHS) model. The method provides spectral accuracy in the velocity domain, which is the highest accuracy achieved by a numerical method for the Boltzmann equation, and the computational complexity of the collisional operator is $O(n^2)$. The method preserves mass, and approximates with spectral accuracy momentum and energy.

In this paper we construct a fractional step deterministic scheme for the time dependent Boltzmann equation, which is based on five main ingredients:

Fractional step in time allows to treat separately the transport and the collision. This approach has the advantage of simplifying the problem, and allows a parallel implementation of the method. As we shall see, the space cells are independent in the collision step, and velocity grid points are independent in the free transport. The use of Strang splitting allows second order accuracy in time. Also, the collision and transport time step can be treated independently, and the latter can be chosen to be smaller than the former.

Fourier-spectral method for the evolution of the collision step allows a very accurate discretization in velocity domain, at a reasonable computational cost [18].

Positive and flux conservative (PFC) finite volume method for the free transport [9] provides a third order (in space) accurate scheme for the evolution of distribution function during the transport step. The scheme is conservative, and it preserves the positivity of the function. It is much less dissipative than ENO and WENO schemes usually used for hyperbolic systems of conservation laws [21,22].

Positive time discretization. A suitable time discretization of the collisional equation is used, which allows a large stability time step, even for problems with considerably small Knudsen number. The time discretization method for the collision step is based on a modified time relaxed scheme [19]. For small Knudsen number, the relaxed time will be chosen in such a way that positivity of the function is essentially preserved.

Multiple resolution. A different resolution will be used in velocity space in the transport and in the collision step. Considering that the collision step is more expensive, and more accurate than the transport step, it is convenient to use more points in velocity space during the transport step. This effect is taken into account in order to optimize the scheme in terms of accuracy and efficiency.

The plan of the paper is the following. In the next section we recall the main properties of the Boltzmann equation. In Section 3, after a general setup, we describe in detail the PFC method for the free transport and the spectral method for the evolution of the collision step. Several numerical issues are discussed at the end of the section. Section 4 is devoted to numerical tests for the space homogeneous BE and for 1D and 2D, time dependent and stationary problems. Finally, in the last section we draw conclusions.

2. The governing equation

In absence of external forces the time evolution of a single component mono atomic gas is governed by the Boltzmann equation (cf. [5])

$$\frac{\partial f}{\partial t} + v \cdot \nabla_x f = \frac{1}{\epsilon} Q(f, f), \quad x, v \in \mathbb{R}^3, \tag{1}$$

where $f = f(t, x, v)$ is a non-negative function describing the distribution of particles which move with velocity v in the position x at time $t > 0$. The number $\epsilon > 0$ is called Knudsen number and is proportional to the mean free path between collisions. In the right-hand side, $Q(f, f)$ is the so-called *collision operator* given by

$$Q(f, f)(v) = Q^+(f, f) - L[f]f \tag{2}$$

with

$$Q^+(f, f) = \int_{\mathbb{R}^3} \int_{S^2} B(|v - v_1|, \theta) f(v') f(v_1') \, d\omega \, dv_1, \tag{3}$$

$$L[f] = \int_{\mathbb{R}^3} \int_{S^2} B(|v - v_1|, \theta) f(v_1) \, d\omega \, dv_1. \tag{4}$$

In the above integrals, v and v_1 are the velocities after the collision of two particles which had the velocities v' and v_1' before the encounter. The deflection angle θ is the angle between $v - v_1$ and $v' - v_1'$.

Here the pre-collision velocities are parameterized by

$$v' = \frac{1}{2}(v + v_1 + |v - v_1|\omega), \quad v_1' = \frac{1}{2}(v + v_1 - |v - v_1| \mid \omega), \tag{5}$$

where ω is a unit vector of the sphere S^2,

$$S^2 = \{\omega \in \mathbb{R}^3, |\omega|^2 = 1\}. \tag{6}$$

The quantities $Q^+(f, f)$ and $L[f]f$ are the gain and loss term, respectively. The precise form of the kernel B, which characterizes the details of the binary interactions, depends on the physical properties of the gas. In the case of inverse kth power forces between particles, the kernel has the form

$$B(|v - v_1|, \theta) = b_\alpha(\theta)|v - v_1|^\alpha, \tag{7}$$

where $\alpha = (k - 5)/(k - 1)$. In particular, we will consider the variable hard sphere(VHS) model [2], i.e., $b_\alpha(\theta) = C_\alpha$ where C_α is a positive constant. The case $\alpha = 0$ is referred to as Maxwellian gas whereas the case $\alpha = 1$ yields the hard sphere gas. Note that in the case of Maxwellian gas the coefficient of the loss term, $L[f]$, does not depend on v. Boltzmann's collision operator has the fundamental properties of conserving mass, momentum and energy

$$\int_{\mathbb{R}^3} Q(f, f) \begin{pmatrix} 1 \\ v \\ |v|^2 \end{pmatrix} \mathrm{d}v = 0, \tag{8}$$

and satisfies the well-known Boltzmann's H-theorem

$$\int_{\mathbb{R}^3} Q(f, f) \log(f) \, \mathrm{d}v \leqslant 0. \tag{9}$$

Boltzmann H-theorem implies that any equilibrium distribution function, i.e., any function f for which $Q(f, f) = 0$, has the form of a locally Maxwellian distribution

$$M(\rho, u, T)(v) = \frac{\rho}{(2\pi T)^{3/2}} \exp\left(-\frac{|u - v|^2}{2T}\right), \tag{10}$$

where ρ, u, T are the density, mean velocity and temperature of the gas

$$\rho = \int_{\mathbb{R}^3} f(v) \, \mathrm{d}v, \quad u = \frac{1}{\rho} \int_{\mathbb{R}^3} v f(v) \, \mathrm{d}v, \quad T = \frac{1}{3\rho} \int_{\mathbb{R}^3} |u - v|^2 f(v) \, \mathrm{d}v. \tag{11}$$

3. The general framework

Let us consider the initial-boundary value problem for the Boltzmann transport equation

$$\frac{\partial f}{\partial t} + v \cdot \nabla_x f + E(t, x) \cdot \nabla_v f = \frac{1}{\epsilon} Q(f, f), \tag{12}$$

$$f(0, x, v) = f_0(x, v),$$

where $x \in \Omega \subset \mathbb{R}^m$, $v \in \mathbb{R}^3$, $t \in [0, T]$. Boundary conditions will be specified in the section on numerical results. Here $E(t, x)$ represents an external drift field acting on the particles. The approach presented in this section can be used for a more general kinetic equation, but in this paper we shall apply it only to the Boltzmann equation of rarefied gas dynamics, where $E \equiv 0$. We discretize time into discrete values t^n, and we denote by $f^n(x, v)$ an approximation of the distribution function $f(t^n, x, v)$. As it is usually done for a kinetic equation like (12), a simple first order time splitting is obtained considering, in a small time interval $\Delta t = [t^n, t^{n+1}]$, the numerical solution of the transport step

$$\frac{\partial f^*}{\partial t} + v \cdot \nabla_x f^* + E(t, x) \cdot \nabla_v f^* = 0,$$
$$f^*(0, x, v) = f^n(x, v),$$
(13)

and the space homogeneous collision step

$$\frac{\partial f^{**}}{\partial t} = \frac{1}{\epsilon} Q(f^{**}, f^{**}),$$
$$f^{**}(0, x, v) = f^*(\Delta t, x, v).$$
(14)

We shall denote by $S_1(\Delta t)$ and $S_2(\Delta t)$ the solution operators corresponding respectively to the transport and collision step, i.e., we can write

$$f^*(\Delta t, x, v) = S_1(\Delta t) f^n(x, v),$$

$$f^{**}(\Delta t, x, v) = S_2(\Delta t) f^*(\Delta t, x, v).$$

The approximated value at time t^{n+1} is then given by

$$f^{n+1}(x, v) = f^{**}(\Delta t, x, v) = S_2(\Delta t) S_1(\Delta t) f^n(x, v).$$
(15)

We assume that S_1 and S_2 represent either exact or at least second order evolution operators in time of transport and collision step, respectively.

A second order scheme for non-stiff problems can be easily derived simply by symmetrizing the first order scheme [24]

$$f^{n+1} = S_1(\Delta t/2) S_2(\Delta t) S_1(\Delta t/2) f^n,$$
(16)

provided every step is solved with a method at least second order accurate in time. Recently, second order splitting algorithms for Boltzmann like equations were also presented in [15]. Although higher order splitting strategies are available, in practice they are seldom used because of stability problems. We remind that second order accuracy for such complex problems is considered "high order" in this field.

In the following two sections we discuss transport and collision steps. As we shall see, the grid step size in time, space and velocity are not directly related by strict stability requirements, and therefore one can benefit from high order accuracy whenever possible. Our final scheme will be overall second order in time, third order in space, and spectrally accurate in velocity.

3.1. The transport step

In this section, we discuss the numerical resolution of the Vlasov equation which characterizes the transport step. To this aim we use an Eulerian method which consists in discretizing the distribution function f on a phase space grid [9].

Let us consider the Vlasov equation written in the form

$$\frac{\partial f}{\partial t} + \text{div}_x(v\, f) = 0. \tag{17}$$

For simplicity, let us restrict ourselves to the following 1D transport equation for $f(t,x)$, even if the PFC reconstruction can be easily generalized to higher dimension using tensor product

$$\partial_t f + \partial_x(u\, f) = 0 \quad \forall (t,x) \in \mathbb{R}^+ \times \mathbb{R}, \tag{18}$$

where u is a constant velocity. Then, the solution of the transport equation at time t^{n+1} reads

$$f(t^{n+1}, x) = f(t^n, x - u\Delta t) \quad \forall x \in \mathbb{R}.$$

Now, let us introduce a finite set of mesh points $\{x_{i+1/2}\}_{i\in I}$ on the computational domain. We will use the notations $\Delta x = x_{i+1/2} - x_{i-1/2}$ (the grid is uniform), $x_i = (x_{i+1/2} + x_{i-1/2})/2$ and $C_i = [x_{i+1/2} - x_{i-1/2}]$. Assume the values of the distribution function are known at time $t^n = n\Delta t$, we compute the new values at time t^{n+1} by integration of the distribution function on each sub-interval. Thus, using the explicit expression of the solution, we have

$$\int_{x_{i-1/2}}^{x_{i+1/2}} f(t^{n+1}, x)\,\mathrm{d}x = \int_{x_{i-1/2}-u\Delta t}^{x_{i+1/2}-u\Delta t} f(t^n, x)\,\mathrm{d}x,$$

then, setting

$$\Phi_{i+1/2}(t^n) = \int_{x_{i+1/2}-u\Delta t}^{x_{i+1/2}} f(t^n, x)\,\mathrm{d}x,$$

we obtain the conservative form

$$\int_{x_{i-1/2}}^{x_{i+1/2}} f(t^{n+1}, x)\,\mathrm{d}x = \int_{x_{i-1/2}}^{x_{i+1/2}} f(t^n, x)\,\mathrm{d}x + \Phi_{i-1/2}(t^n) - \Phi_{i+1/2}(t^n). \tag{19}$$

The evaluation of the average of the solution over $[x_{i-1/2}, x_{i+1/2}]$ allows to ignore fine details of the exact solution which may be costly to compute. The main step is now to choose an efficient method to reconstruct the distribution function from the cell average on each cell C_i. In [8], the author used simple linear interpolation. Unfortunately this approach does not give a positive scheme and does not control spurious oscillations. Here, we will consider a reconstruction via primitive function preserving positivity and maximum values of f. Let $F(t^n, x)$ be a primitive of the distribution function $f(t^n, x)$, if we denote by

$$f_i^n = \frac{1}{\Delta x} \int_{x_{i-1/2}}^{x_{i+1/2}} f(t^n, x)\,\mathrm{d}x,$$

then $F(t^n, x_{i+1/2}) - F(t^n, x_{i-1/2}) = \Delta x f_i^n$ and

$$F(t^n, x_{i+1/2}) = \Delta x \sum_{k=0}^{i} f_k^n = w_i^n.$$

In the sequel, the time variable t^n only acts as a parameter and will be omitted. A reconstruction method allowing to preserve positivity and maximum principle can be obtained using slope correctors. First we build an approximation of the primitive on the interval $[x_{i-1/2}, x_{i+1/2}]$ using the stencil $\{x_{i-3/2}, x_{i-1/2}, x_{i+1/2}, x_{i+3/2}\}_{i\in I}$,

$$\tilde{F}_h(x) = w_{i-1} + (x - x_{i-1/2})f_i + \frac{1}{2\Delta x}(x - x_{i-1/2})(x - x_{i+1/2})[f_{i+1} - f_i]$$
$$+ \frac{1}{6\Delta x^2}(x - x_{i-1/2})(x - x_{i+1/2})(x - x_{i+3/2})[f_{i+1} - 2f_i + f_{i-1}],$$

where we used the relation $w_i - w_{i-1} = \Delta x f_i$. Thus, by differentiation, we obtain a third order accurate approximation of the distribution function on the interval $[x_{i-1/2}, x_{i+1/2}]$,

$$\tilde{f}_h(x) = \frac{d\tilde{F}_h}{dx}(x)$$
$$= f_i + \frac{1}{6\Delta x^2}\left[2(x - x_i)(x - x_{i-3/2}) + (x - x_{i-1/2})(x - x_{i+1/2})\right](f_{i+1} - f_i) - \frac{1}{6\Delta x^2}\left[2(x - x_i)(x - x_{i+3/2})\right.$$
$$\left. + (x - x_{i-1/2})(x - x_{i+1/2})\right](f_i - f_{i-1}).$$

In order to satisfy a maximum principle and to avoid spurious oscillations we introduce the slope correctors

$$f_h(x) = f_i + \frac{\epsilon_i^+}{6\Delta x^2}\left[2(x - x_i)(x - x_{i-3/2}) + (x - x_{i-1/2})(x - x_{i+1/2})\right](f_{i+1} - f_i)$$
$$- \frac{\epsilon_i^-}{6\Delta x^2}\left[2(x - x_i)(x - x_{i+3/2}) + (x - x_{i-1/2})(x - x_{i+1/2})\right](f_i - f_{i-1}) \tag{20}$$

with

$$\epsilon_i^\pm = \begin{cases} \min\left(1; 2f_i/(f_{i\pm1} - f_i)\right) & \text{if } f_{i\pm1} - f_i > 0, \\ \min\left(1; -2(f_\infty - f_i)/(f_{i\pm1} - f_i)\right) & \text{if } f_{i\pm1} - f_i < 0, \end{cases} \tag{21}$$

where $f_\infty = \max_{j \in I}\{f_j\}$.

It is easy to check that the approximation of the distribution function $f_h(t^n, x)$ previously constructed satisfies (see [9] for the proof)

- conservation of the average: for all $i \in I$, $\int_{x_{i-1/2}}^{x_{i+1/2}} f_h(t^n, x)\,dx = \Delta x f_i^n$,
- maximum principle: for all $x \in (x_{\min}, x_{\max})$, $\quad 0 \leqslant f_h(t^n, x) \leqslant f_\infty$
- consistency:

$$\int_{\mathbb{R}} |f_h(t^n, x) - \tilde{f}_h(t^n, x)|\,dx \leqslant C\Delta x,$$

where $\tilde{f}_h(t^n, x)$ is the third order approximation previously defined.

3.2. Spectral approximation of the collision operator

We consider now the space homogeneous Boltzmann equation in each cell

$$\frac{\partial f}{\partial t} = Q^+(f, f) - L[f]f, \tag{22}$$

with Q^+ and L given by Eqs. (3) and (4). To keep notation simple, we have fixed $\epsilon = 1$. A simple change of variables permits to write

$$Q^+(f, f) = \int_{\mathbb{R}^d} \int_{S^{d-1}} B(|g|, \theta)f(v')f(v_1')\,d\omega\,dg, \tag{23}$$

$$L(f) = \int_{\mathbb{R}^d} \int_{S^{d-1}} B(|g|, \theta) f(v - g) \, d\omega \, dg, \tag{24}$$

where $g = v - v_1$ and then

$$v' = v - \frac{1}{2}(g - |g|\omega), \quad v_1' = v - \frac{1}{2}(g + |g|\omega). \tag{25}$$

The dimension of velocity space is $d = 3$. However we consider the case of $d = 2$, i.e., the Boltzmann equation with 2D in velocity, because the realistic case of 3D in velocity requires a more efficient implementation and a more powerful computer than the one available.

The Fourier approximation is based on the observation that if a distribution function f is well approximated by a function with compact support in velocity space (say a ball centered at the origin with radius R), then it can be approximated by a periodic function in velocity space, whose period $2V$ is proportional to the size of the support: $V = (3 + \sqrt{2})R/2$ (see Fig. 1 and [18] for details).

To simplify the notation we assume that the half period is $V = \pi$ and hence $R = \lambda\pi$ with $\lambda = 2/(3 + \sqrt{2})$. Hereafter, we used just one index to denote the 3D sums with respect to the vector $k = (k_1, k_2, k_3) \in \mathbb{Z}^3$, hence we set

$$\sum_{k=-N}^{N} = \sum_{k_1, k_2, k_3 = -N}^{N}.$$

The approximate function f_N is represented as the truncated Fourier series

$$f_N(v) = \sum_{k=-N}^{N} \hat{f}_k e^{ik \cdot v}, \tag{26}$$

$$\hat{f}_k = \frac{1}{(2\pi)^3} \int_{[-\pi,\pi]^3} f(v) e^{-ik \cdot v} \, dv.$$

By inserting Eq. (26) into Eq. (22) and imposing orthogonality of the residual with all trigonometric polynomials of degree $\leqslant N$, one obtains the following evolution equations:

$$\frac{\partial \hat{f}_k}{\partial t} = \sum_{m=\max(-N, k-N)}^{\min(N, k+N)} \hat{f}_{k-m} \hat{f}_m (\hat{B}(k - m, m) - \hat{B}(m, m)) \tag{27}$$
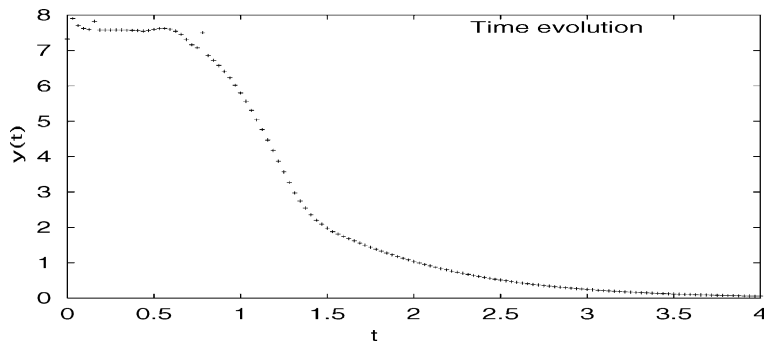

Fig. 1. Space homogeneous case: time evolution of the value $\mu(t)$.

with the initial condition

$$\hat{f}_k(0) = \frac{1}{(2\pi)^3} \int_{[-\pi,\pi]^3} f_0(v) e^{-ik\cdot v} \, dv, \tag{28}$$

where the *kernel modes* $\hat{B}(l,m)$ are given by

$$\hat{B}(l,m) = \int_{\mathscr{B}(0,2\lambda\pi)} \int_{S^2} B(|g|,\theta) \exp\left\{ -ig \cdot \frac{(l+m)}{2} - i|g|\omega \cdot \frac{(m-l)}{2} \right\} d\omega \, dg. \tag{29}$$

The evaluation of the right-hand side of Eq. (27) requires exactly $\mathcal{O}(N^6)$ operations. We emphasize that the usual cost for a method based on N^3 parameters for f in the velocity space is $\mathcal{O}(N^6 M)$ where n_a is the number of angle discretizations. The loss term on the right hand side is a convolution sum and thus transform methods allow this term to be evaluated only in $\mathcal{O}(N^3 \log N)$ operations. Hence the most expensive part of the computation is represented by the gain term.

Explicit expression for the kernel modes for Variable Hard Spheres in 3D can be obtained [18].

For the 2D VHS model one has

$$\hat{B}(l,m) = C_\alpha 4\pi^2 (2\pi\lambda)^{2+\alpha} F_\alpha(\xi,\eta)$$

with

$$F_\alpha(\xi,\eta) = \int_0^1 r^{1+\alpha} J_0(\xi r) J_0(\eta r) dr, \tag{30}$$

where $\xi = |l+m|\lambda\pi$, $\eta = |l-m|\lambda\pi$, $r = |g|/2\lambda\pi$, and J_0 is the Bessel function of order 0. Note that each kernel mode can be computed as a 1D integral and stored in an array.

The spectral approximation provides a consistent description of the space homogeneous Boltzmann equation, which preserves mass, but not energy and momentum. The scheme is spectrally accurate for smooth solutions, thus providing spectral accuracy in the conservation of momentum and energy as well. The properties of the scheme are analyzed in detail in [18].

3.3. Time discretization

The time discretization of the transport step has been described in Section 3.1. Here we focus on the time evolution of the collision step. Let Δt denote the time step of the transport phase. Our goal is to solve, in each cell, the space homogeneous Boltzmann equation

$$\frac{\partial f^*}{\partial t} = \frac{1}{\epsilon} Q(f^*, f^*),$$

$$f^*(0,v) = f^n(v),$$

where, for simplicity, we drop the space dependence. One could use any second order time discretization, such as a Runge–Kutta method, with the same time step, Δt, used for the convection step, for the ordinary differential system of the Fourier modes, (27). If the time step is too large (for accuracy or stability reasons), then a smaller time step, $\Delta t_c < \Delta t$, can be used during this phase. Since each cell is independent, Δt_c may depend on the cell. If $\Delta t_c \ll \Delta t$, then a multi-step scheme can be used to improve efficiency and accuracy. With standard methods such as Runge–Kutta or multi-step, it is difficult to control positivity of the solution. Here we propose a time discretization which provides essential positivity of the distribution function, and allows the use of rather large time step, even in regimes in which the Knudsen number is quite

small. The schemes that we use are based on a variation of time relaxed (TR) schemes [19], which have been effectively used in the development of Monte-Carlo methods suitable for a very wide range of Knudsen number. We briefly recall here the idea behind the TR schemes.

Let us consider an equation of the form

$$\frac{\partial f}{\partial t} = \frac{1}{\epsilon}[P(f,f) - \mu f], \quad f(0,v) = f_0(v), \tag{31}$$

where $\mu \neq 0$ is a constant and P a positive bilinear operator. The Boltzmann equation for Maxwell molecules has the above form, with $Q^+(f,f) = P(f,f)$, and $L[f] = \mu$.

A formal representation of the solution of the Cauchy problem (31) is given by the so called Wild sum expansion (see [19] and [26]),

$$f(t,v) = \sum_{k=0}^{\infty}(1-\tau)\tau^k f_k(v), \tag{32}$$

where $\tau = (1 - e^{-\mu t/\epsilon})$ is the reduced time. The functions f_k, given by the recurrence formula

$$f_{k=0}(v) = f_0(v), \quad f_{k+1}(v) = \frac{1}{k+1}\sum_{h=0}^{k}\frac{1}{\mu}P(f_h, f_{k-h}), \qquad k = 0, 1, \ldots, \tag{33}$$

satisfy the property

$$\lim_{k\to\infty} f_k(v) = M(v), \tag{34}$$

where $M(v)$ is the Maxwellian, satisfying $Q(M,M) = 0$.

Representation (32) and property (34) suggest the use of a truncation of series (32) as a numerical scheme for time discretization, or, better, of a generalization of such a truncated series, of the form

$$f^{n+1} = \sum_{k=0}^{m} A_k f_k + A_{m+1}M, \tag{35}$$

where the coefficients f_k are given by Eq. (33) using $f_0 = f^n(v)$. The weights $A_k = A_k(\tau)$ are non-negative functions that satisfy some consistency and conservation conditions. Further conditions on the coefficients will ensure *asymptotic preservation* (AP), i.e., in the limit of vanishing ϵ, the distribution function is projected by the scheme into the Maxwellian $M(v)$ (see [19] for details). A choice of functions which satisfies the previous requirements is, for example,

$$A_k = (1-\tau)\tau^k, \ \ k = 0, \ldots, m-1, \quad A_m = 1 - \sum_{k=0}^{m-1} A_k - A_{m+1}, \quad A_{m+1} = \tau^{m+2}, \tag{36}$$

which corresponds to take $f_{m+1} = f_m, f_k = M, k \geqslant m + 2$ in (32). However, other choices are possible and it is an open problem the determination of the *optimal* set of functions A_k that satisfies the previous requirements and guarantees the most accurate approximation.

The Boltzmann equation for Maxwell molecules has the form (31), with $P(f,f) = Q^+(f,f)$. In order to apply the same discretization to a more general BE, we can proceed as follows. We write the Boltzmann equation in the form (31), with

$$P(f,g) = Q^+(f,g) + \frac{1}{2}(\mu(f+g) - L[f]g - L[g]f),$$

where the operator P is written in a symmetric form. If we choose

$$\mu \geqslant L[f](v) \quad \forall v \in \mathbb{R}^3, \tag{37}$$

then $P(f,f)$ is a positive symmetric operator. However, in general $L(v)$ is an unbounded function, and therefore a constant μ satisfying (37) does not exist. Even if we consider that the discrete velocities lie in a bounded domain $\Omega_v = [-V,V]^3$, a choice of μ satisfying Eq. (37) may lead to excessive numerical viscosity, as is evident from standard truncation analysis.

Ideally, one should choose the smallest value of μ that guarantees positivity of operator P. This should be obtained, for a given function $f(v)$, by imposing that

$$\min_{v \in \Omega_v}[Q^+(v) + (\mu - L(v))f(v)] = 0. \tag{38}$$

A first order (non-AP) TR scheme has the structure

$$f^{n+1}(v) = A_0(\tau)f^n(v) + A_1(\tau)f_1(v)$$

with $f_1 = P(f^n, f^n)/\mu$. Because of positivity of the coefficients $A_0(\tau)$ and $A_1(\tau)$, if $P(f,f)$ is positive, then the scheme is positive.

Condition (38) is not practical, since the region of phase space Ω_v near the edge is not physically representative, because of the approximation of the distribution function by a periodic function in velocity. A better choice is obtained by computing a critical constant μ_c as

$$\mu_c = \max_{v \in \Omega_c}\left(L(v) - \frac{Q_+}{f}\right), \tag{39}$$

where $\Omega_c \subset \Omega_v$ is a smaller region, for example, $\Omega_c = [-V/2, V/2]^3$. Then the constant μ is computed as $\mu = C\mu_c$, where C is a safety factor of order one. In all our calculations we used the value $C = 3/2$, which we found a good compromise between numerical positivity and numerical viscosity.

These practical criteria deserve further analysis. We have to keep in mind that the spectral scheme itself does not preserve positivity rigorously [18]. However, the lack of positivity is very small, and can be neglected for all practical purposes. Even if positive spectral schemes can be obtained, as shown in [18] and [17], they are not practical, because of the lack of accuracy and excessive smoothing.

Accuracy requires a small value of $\mu\Delta t/\epsilon$. If μ is kept constant, independently of ϵ, then the time step becomes exceedingly small for small values of ϵ, and the method becomes inefficient. The approach that we outlined above allows rather large time steps, even for small values of ϵ. The reason for this is that when ϵ is small, then gain and loss terms balance each other, and therefore the quantity μ computed as above becomes small. It can be shown in fact that for small values of ϵ, μ scales with ϵ, and the ratio μ/ϵ remains bounded.

With these considerations in mind, we maintain the same criterion for the evaluation of the optimal μ, even for higher order TR schemes.

A second order (non-AP) TR scheme has the structure

$$f^{n+1}(v) = A_0(\tau)f^m(v) + A_1(\tau)f_1(v) + A_2(\tau)f_2(v),$$

with $f_2(v) = P(f^n, f_1)$. The constant μ is computed as above, $\mu = 3/2\mu_c$, with μ_c given by (39). For all practical purpose the scheme can be considered positive, although it is not rigorously positive.

3.3.1. Parallelization algorithm

Let us denote by f^n (resp. f^*) the matrix $(f_{i,j}^n)$ (resp. $(f_{i,j}^*)$) corresponding to the values of the discrete distribution function at time t^n (resp. $S_1(\Delta t)f^n$), where i represents the index of the physical space mesh and

j the index of the velocity space. We note that the big amount of work is performed during steps (13) and (14). Therefore, we will focus on the parallelization of these computations. To do this we observe that the operator $S_1(\Delta t)$ (resp. $S_2(\Delta t)$) only acts on rows of $(f_{i,j}^n)$ (resp. on columns of $(f_{i,j}^*)$). Thus, for the step $S_1(\Delta t)$ if we assume that data are distributed by row on each processor, no communications are required and similarly, for the other step $S_2(\Delta t)$ a storage by column does not involve any communication at all. The link between the two steps is done through a transposition of f^*.

Following this idea, we present a simple parallel algorithm [7], starting with 1D band distribution f^n along v-direction.

Algorithm 1. For each time step Δt:
(a) Compute the matrix f^* using $S_1(\Delta t)$ from values f^n. The storage by rows avoids local communications for this step.
(b) Distribute the matrix f^* into the matrix transposed f^{*^T} in order to get a 1D band distribution along x-direction.
(c) Apply $S_2(\Delta t)$ to f^{*^T} for solving Eq. (14) over a time step of Δt. The storage by columns avoids local communications for this step.
(d) Redistribute matrices f^{n+1^T} into matrix f^{n+1} in order to get a 1D band distribution along v-direction.
End.

In this case, we notice that with our parallel algorithm, communications only occur during the two data redistributions phases. In other words, the algorithm falls into phases of computations without any communication and phases of communications without any computation.

3.3.2. Multi-resolution algorithm

It is easy to check that the computational cost of the transport step (13) is of order $O(N_x N_v)$, where N_x (resp. N_v) is the number of points in x-direction (resp. v-direction), whereas the numerical approximation of the integral collision operator (14) requires an amount of work of order $O(N_x N_{\text{modes}}^2)$, where N_{modes} represents the total number of modes in velocity. Then, this last step is much more time consuming than the first one. However, the Fourier approximation gives an accurate approximation due to the spectral accuracy [16], whereas the transport part is only third order. In this section, we then propose a simple algorithm to reduce the computational time keeping good accuracy. It is based on multilevel resolution: the transport equation is solved on a fine grid $N_x \times N_v$, whereas the collision operator is treated using a smaller number of modes. The link between the two grids is achieved through trigonometric interpolation, which preserves the good accuracy of the spectral method.

Algorithm 2. For each time step Δt:
1. Compute the first approximation f^* by $S_1(\Delta t)$ using f^n on the fine grid with a cost $O(N_x N_v)$.
2. Compute a Fourier approximation of f^* using FFT with a cost $O(N_x N_v \log(N_v))$
3. Neglect highest frequencies of $(\hat{f}_k^*)_k$, keeping only N_{modes} terms, and compute $\hat{f}^{**}$ the approximated solution of $S_2(\Delta t)f^*$ in the Fourier space, with a cost $O(N_x N_{\text{modes}}^2)$, where $N_{\text{modes}} \ll N_v$.
4. Use a trigonometric interpolation to get f^{n+1} on the fine grid with a cost of order $O(N_x N_v \log(N_v))$.
End.

4. Numerical tests

In this section, we present a large variety of test cases showing the effectiveness of our method to get an accurate solution of the Boltzmann equation. We first give a classical example, which illustrates the

property of the time relaxed scheme. Then, we give several results to compare our scheme with the well known Monte-Carlo method for the Boltzmann equation. Finally, we present an interesting result in the $2 + 2$-dimensional phase space proving the high accuracy of our method, which is able to reproduce small effects (ghost effects). In our space dependent tests we used a 2D model of the Boltzmann equation in velocity space. Realistic simulations with a full 3D model in velocity space require more powerful computer and faster algorithms for storage and retrieval of the Fourier modes of the collision kernel.

4.1. Space homogeneous problems

This test is used to find the good strategy for the time discretization. Let us consider the space homogeneous 2D-Boltzmann equation for hard sphere molecules. The initial data are chosen as the sum of two Maxwellian functions

$$f_0(v) = \frac{1}{2} \frac{5}{(2\pi v_{\mathrm{th}}^2)} \left[\exp\left(-\frac{|v - v_1|^2}{2v_{\mathrm{th}}^2} \right) + \exp\left(-\frac{|v - v_2|^2}{2v_{\mathrm{th}}^2} \right) \right], \quad v \in \mathbb{R}^2,$$

with $v_1 = (2, 1)$, $v_2 = (-2, -1)$ and the thermal velocity is $v_{\mathrm{th}} = 1$. The final time of the simulation is $T_{\mathrm{end}} = 5$, which is very closed to the stationary state. We first compute an accurate solution by the spectral method using 64^2 modes and a fourth order Runge–Kutta scheme for the time discretization. In Fig. 1, we represent the time evolution of the constant $\mu(t)$, which allows us to rewrite the Boltzmann operator as the sum of a positive operator and a loss term

$$\mu(t) = \frac{3}{2} \max_{v \in \Omega_c} \left(L(v) - \frac{Q_+}{f} \right).$$

The solution is computed from time t^n to time $t^{n+1} = t^n + \Delta t$ using a first order time-relaxed scheme preserving asymptotic behavior

$$f^{n+1}(v) = A_0(\tau) f^n(v) + A_1(\tau) f_1(v) + A_2(\tau) M(v)$$

with $f_1 = Q^+(f^n, f^n)/\mu$, whereas A_0, A_1 and A_2 are given by (36).

The distribution function is initially far from the equilibrium and the value of μ is large. Then, the time going on, the solution is closer to the Maxwellian corresponding to the stationary state, i.e., $Q(f, f) = 0$ and the value of $\mu(t)$ goes to zero.

Finally, we compute a numerical solution with an adaptive time step $\Delta t = \tau/\mu(t)$ when τ is fixed. The results are reported in Table 1. This solution is compared with one computed with a fixed time step $\Delta t = T/n_{\mathrm{Tot}}$, where T is the final time and n_{Tot} the total number of iterations. Then, the value $\varepsilon^{(1)}$ represents the numerical error with a fixed time step

$$\varepsilon^{(1)} = \max_{t \in (0,T)} \{ \|f_{\Delta t}(t) - f_{\mathrm{exa}}(t)\|_{L^1}, \ \Delta t = T/n_T \};$$

we also report the numerical error $\varepsilon^{(2)}$ given by

$$\varepsilon^{(2)} = \max_{t \in (0,T)} \{ \|f_{\Delta t}(t) - f_{\mathrm{exa}}(t)\|_{L^1}, \ \Delta t = \tau/\mu(t) \}.$$

We first observe that the solution obtained by the second algorithm when τ is fixed is more accurate compared to the solution obtained with a fixed time step using the same number of iterations. Moreover, in view of Table 1, the numerical error $\varepsilon^{(2)}$ highly depends on the value of $\tau = \mu(t)\Delta t$. Indeed, when τ is close to zero, the second order time relaxed scheme computes an accurate solution and $\varepsilon^{(2)}$ is small, and when τ is close to the final time T corresponding to the stationary state, the time relaxed scheme com-

Table 1
Space homogeneous case: error with respect to the time discretization

$\tau = \mu(t)\Delta t$	n_{Tot}	Numerical error $\varepsilon^{(1)}$ with a fixed $\Delta t = T/n_{\text{Tot}}$	Numerical error $\varepsilon^{(2)}$ with $\Delta t = \tau/\mu(t)$
0.010	50	0.0036	0.002
0.025	20	0.0080	0.007
0.050	11	0.0160	0.014
0.100	08	0.0300	0.025
0.200	07	0.0520	0.045
0.500	05	0.2000	0.090
1.000	03	XXXX	0.150
3.000	02	XXXX	0.040
5.000	01	XXXX	0.006

The first colum represents the values of $\tau = \mu\Delta t$, the second one represents the number of time step n_{Tot} corresponding to τ, the third one is the error $\varepsilon^{(1)}$ computed from a fixed time step $\Delta t = T/n_{\text{Tot}}$ and the fourth one is the error $\varepsilon^{(2)}$ with a time step $\Delta t = \tau/\mu(t)$ (τ is fixed).

putes a projection of the distribution function on the corresponding Maxwellian, then the value of $\varepsilon^{(2)}$ is also small.

In conclusion the time step Δt has to be computed with respect to $\mu(t)$ avoiding intermediate values of τ: from time t^n to time $t^{n+1} = t^n + \Delta t$, the time step is computed as follows:

if $\tau = \Delta t \mu(t^n) \notin [\tau_{\min}, \tau_{\max}]$, **then** the time step Δt_n is set to $\tau/\mu(t^n)$,
else a smaller time step is computed $\Delta t_n = \tau_{\min}/\mu(t^n)$.

For practical calculation, we have fixed $\tau_{\min} = 1/10$ and $\tau_{\max} = 5$, which is a good compromise between accuracy and reasonable computational cost.

4.2. Approximation of smooth solutions

This test is used to evaluate the order of accuracy of the algorithm. Let us consider a smooth initial data

$$f_0(x,v) = (1 + \beta \cos(k_0 x)) \exp(-v^2/2), \quad (x,v) \in [0,L] \times \mathbb{R}^2,$$

with $\beta = 0.1$, $k_0 = 1/2$, $L = 4\pi$ and assume periodic boundary conditions in x. Numerical solutions are computed from different phase space meshes (see Table 2) and an estimation of the relative error in L^1 norm is given by

$$\varepsilon_{2h} = \max_{t \in (0,T)}(\|f_h(t) - f_{2h}(t)\|_1)/\|f_0\|_1,$$

where f_h represents the approximation computed from a grid of order h. The numerical scheme is said to be pth order if

$$\varepsilon_{2h} \leqslant C(f)h^p, \quad 0 < h \ll 1.$$

Table 2
Approximation of smooth solutions: discrete relative error norm for different grid sizes

Numerical parameters	Relative l^1 error norm	$\varepsilon_{2h}/\varepsilon_h$
$n_x = 032$, $n_{v_x} = n_{v_y} = 08$, $\Delta t = 0.100$	$\varepsilon_{4h} = 0.3835$	5.20
$n_x = 064$, $n_{v_x} = n_{v_y} = 16$, $\Delta t = 0.050$	$\varepsilon_{2h} = 0.0738$	4.35
$n_x = 128$, $n_{v_x} = n_{v_y} = 32$, $\Delta t = 0.025$	$\varepsilon_h = 0.0169$	X

The convergence rate estimate is in good agreement with one expected by the theory since the scheme is second order; even if the collision operator approximation is given by spectral accuracy in v and the transport step is third order accurate in x, the time splitting scheme is only second order. Note that the approximation obtained with the coarse grid in velocity $n_{v_x} = n_{v_y} = 8$ is poorly accurate, which gives a large rate $\epsilon_{4h}/\epsilon_{2h} = 5.2$ because the error induced by the collision operator approximation is dominant. But with a refined grid we get the good rate of convergence.

4.3. Riemann problem: time dependent solutions

This test deals with the numerical solution of the non-homogeneous $1D \times 2D$ Boltzmann equation for hard sphere molecules ($\alpha = 1$). We present some results for 1D Riemann problem and compare them with the numerical solution obtained by the Monte-Carlo scheme. The Monte-Carlo results are obtained by second order AP TRMC scheme (see [19]).

Let us note that the accuracy of the Monte-Carlo solution is improved by performing averages of the solution itself by repeating the calculation several times with different seeds in the random number generator, and averaging the solution over the different runs. Then, we have computed an approximation for different Knudsen numbers, from rarefied regime up to the fluid limit. The solution in the hydrodynamic limit is also compared with the numerical solution of Euler system, which is obtained by Nessyahu–Tadmor scheme [14] using a large number of points ($n_x = 1600$). The initial data are given by

$$(\rho_l, u_l, T_l) = (1, 0, 1) \qquad \text{if } 0 \leqslant x \leqslant 0.5,$$
$$(\rho_r, u_r, T_r) = (0.125, 0, 0.25) \quad \text{if } 0.5 < x \leqslant 1.$$

In Figs. 2 and 3 we plot the results obtained in the rarefied regime ($\epsilon = 10^{-1}, 10^{-2}$) using the S-PFC scheme and the time relaxed Monte-Carlo (TRMC) method. The TRMC method is used with 100 cells in x containing 100 particles per cell (in the cells at the right of the discontinuity in the initial condition) whereas the S-PFC scheme is used with 64 points in x and the size of the velocity grid is 64×64 points for the transport and the total number of modes 32×32. We observe that the two solutions are in this case very comparable even if small oscillations, due to the statistical noise, persist. Concerning the computational time on one processor, the S-PFC scheme is more efficient than Monte-Carlo in this situation because the averaging highly increases the computational time (see Table 3). Let us note that in the two cases (Monte-Carlo and spectral methods), the Time Relaxed scheme allows to use a large variety of Knudsen number ($\epsilon = 10^{-1}$, 10^{-2}) without increasing the computational cost. Finally, the computational time of the S-PFC scheme can be highly reduced using the parallel algorithm presented before.

We remark here that the solution to the Riemann problem for the equation with a given value of ϵ can be obtained by scaling space and time by ϵ and setting $\epsilon = 1$, therefore the change in ϵ is a convenient way to perform a change in time and space grid. Here the purpose is to show that accurate results can be obtained with our scheme with an under resolved grid, i.e., with a grid that resolves macroscopic variations but not the mean free path.

We also give the result of the computations close to the Euler limit ($\epsilon = 10^{-4}$) using 128 space cells for the S-PFC method. In this case, a smaller time step ($\Delta t = 0.001$) is needed to keep good accuracy, which increases the computational time, while a small time step for the TRMC method does not influence the numerical solution due to the low order (in space) of the Monte-Carlo scheme (see Table 3). For this reason a large time step is used, which explains the best computational cost of the TRMC scheme.

Finally, the profiles obtained with TRMC and S-PFC methods are reported in Fig. 4. The use of first order scheme (in space) for the transport for the TRMC scheme is clearly not sufficient to give accurate results. On the opposite, using a small time step ($\Delta t = 0.001$), an accurate solution is obtained by the S-PFC method, which is much less diffusive.
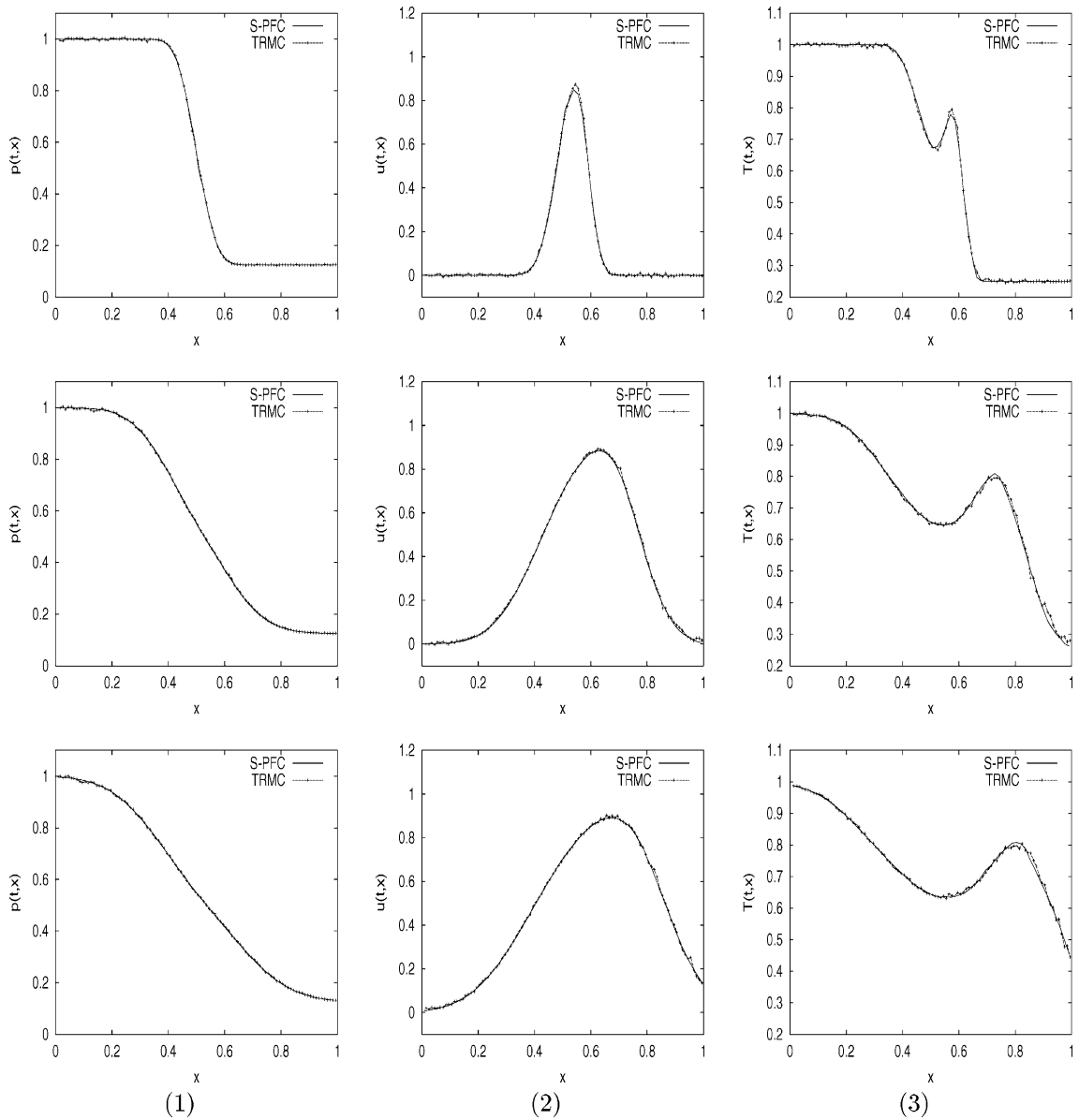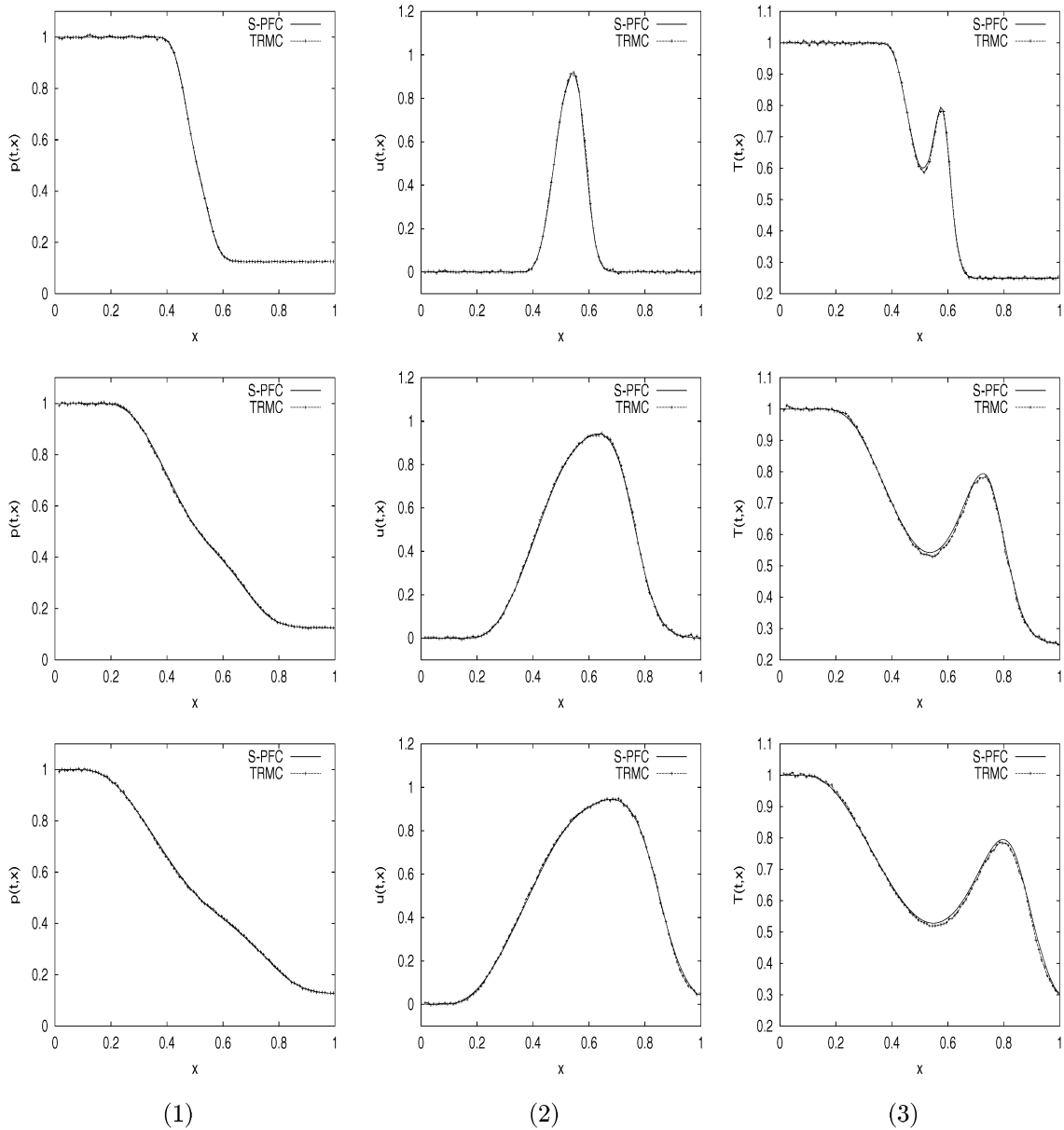
Fig. 2. Riemann problem ($\epsilon = 10^{-1}$): evolution of (1) the density ρ, (2) mean velocity u and (3) temperature T at time $t = 0.05$, 0.15, 0.20.

4.4. Shock profile: stationary solutions

Now we present numerical results for 1D stationary shock-profiles for different Knudsen number and compare the solution with one obtained by the Monte-Carlo method (second order TRMC). We use the same numerical configuration as for the previous test, except that for the Monte-Carlo solution we use 200 cells, and 200 particles per cell at the right of the discontinuity in the initial condition.

Fig. 3. Riemann problem ($\epsilon = 10^{-2}$): evolution of (1) the density ρ, (2) mean velocity u and (3) temperature T at time $t = 0.05, 0.15, 0.20$.

The gas is initially at the upstream equilibrium state in the left half-space and in the downstream equilibrium state in the right-half space. The upstream state are determined from downstream state using the Rankine–Hugoniot relations [25]. In the present calculations, the downstream state is characterized by

$$\rho^r = 1, \quad T^r = 1, \quad M = 3,$$

Table 3
Riemann problem: the first column represents the value of Knudsen numbers ϵ, the second one is the computational time obtained for the TRMC scheme and the third one is the computational time for the third order PFC scheme coupled with the spectral method for the collision operator

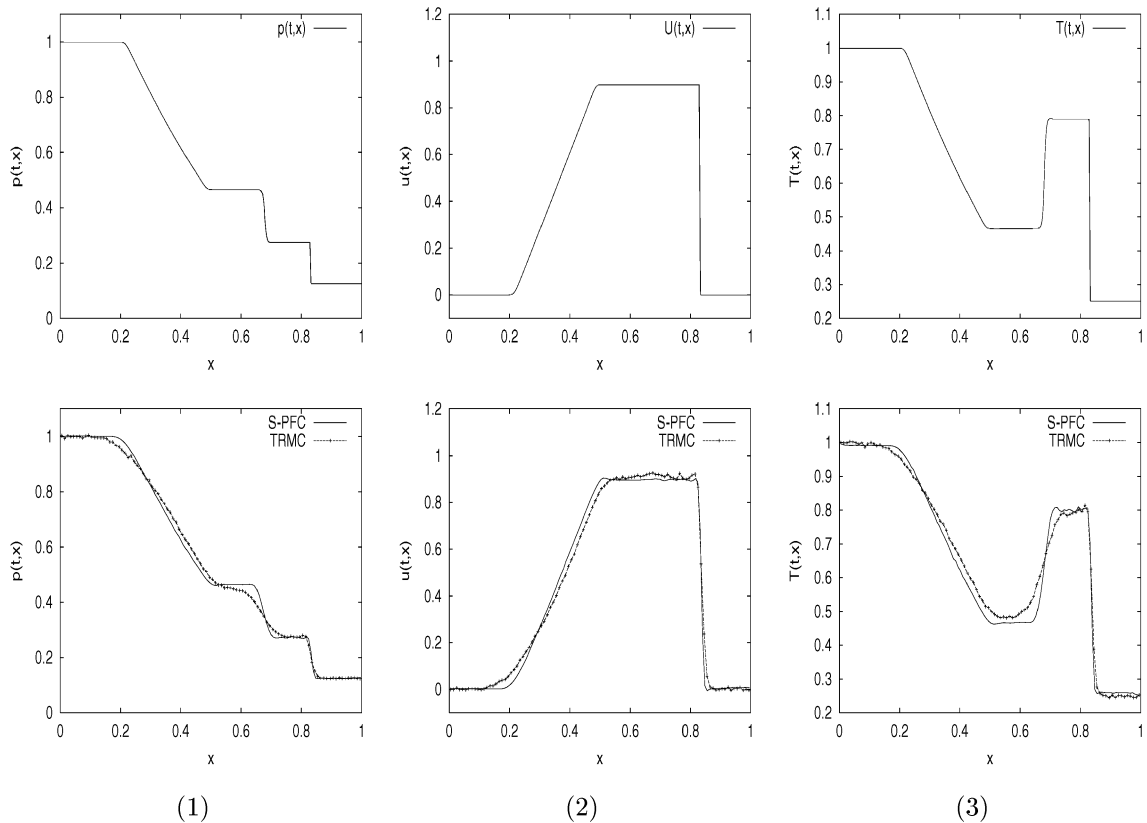|	TRMC	S-PFC
$\epsilon = 10^{-1}$	17 mn 25 s	10 mn 50 s
$\epsilon = 10^{-2}$	17 mn 25 s	10 mn 50 s
$\epsilon = 10^{-4}$	17 mn 25 s	44 mn 20 s

(1)   (2)   (3)

Fig. 4. Riemann problem ($\epsilon = 10^{-4}$): (1) the density ρ, (2) mean velocity u and (3) temperature T at time $t = 0.20$ obtained by the central scheme for Euler equations (up) and by S-PFC and TRMC methods for Boltzmann equations.

where M is the Mach number of the shock. The downstream mean velocity is then given by

$$(u_x^r, u_y^r) = (-M\sqrt{\gamma T}, 0)$$

with $\gamma = 2$ since we have considered a 2D monoatomic gas in velocity space.

The results of the computation are shown in Figs. 5 and 6. On the one hand, we compute a solution using the S-PFC scheme (128 cells in space and 32×32 modes in velocity) up to time $t = 0.2$, so that the profile is practically stationary. On the other hand, Monte-Carlo calculations (TRMC) are performed by time-averaging the numerical solution after large enough time ($t = 0.2$). We observe that there is a good agreement between the TRMC and S-PFC method. In particular, both schemes are able to compute sharp shocks for very small values of ϵ.
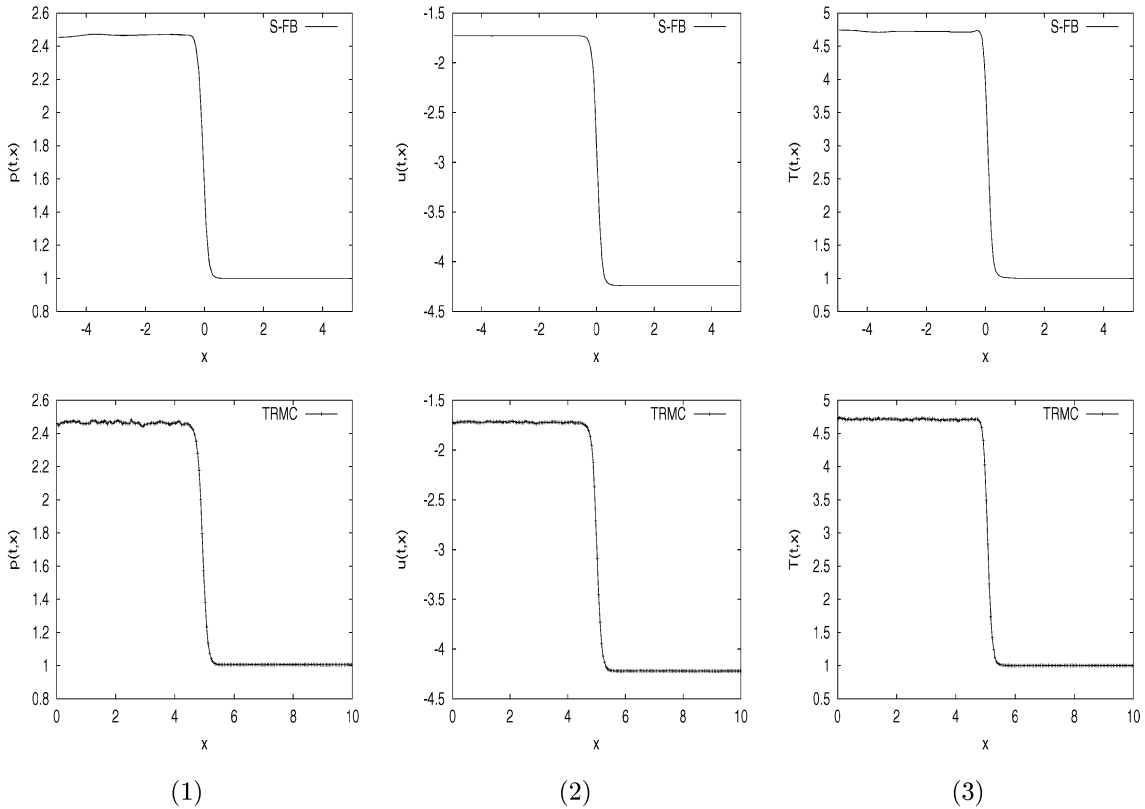
Fig. 5. Shock profiles ($\epsilon = 10^{-1}$): (1) the density ρ, (2) mean velocity u and (3) temperature T obtained by the S-PFC method (up) and by the TRMC method (bottom).

As in the case of the Riemann problem, a small ϵ here means that the shock is under resolved. Our scheme is able to capture the shock even in this case.

4.5. Four $(2+2)$-dimensional Boltzmann equation: the ghost effect

Consider a gas between two plates at rest in a finite domain. In this situation, the stationary state at a uniform pressure (the velocity is equal to zero and the pressure is constant) is an obvious solution of the Navier–Stokes equations; the temperature field is determined by the heat conduction equation [23]

$$u = 0, \quad \rho T = C, \quad -\nabla_x \cdot (T^{1/2} \nabla_x T) = 0.$$

According to the Hilbert expansion with respect to the Knudsen number *Kn*, the density and temperature fields in the continuum limit are affected by the velocity field, which is of order one with respect to *Kn*. Finally, the heat conduction equation, although extracted from the incompressible Navier–Stokes system, is not appropriate in a whole class of situations, in particular when isothermal surfaces are not parallel, thereby giving rise to "ghost effects".

In this section, we will show that the numerical solution agrees with one obtained by the asymptotic theory and not with the one obtained from the heat conduction equation; this result is a confirmation of the validity of the asymptotic theory. This problem has been already studied from the numerical point of view
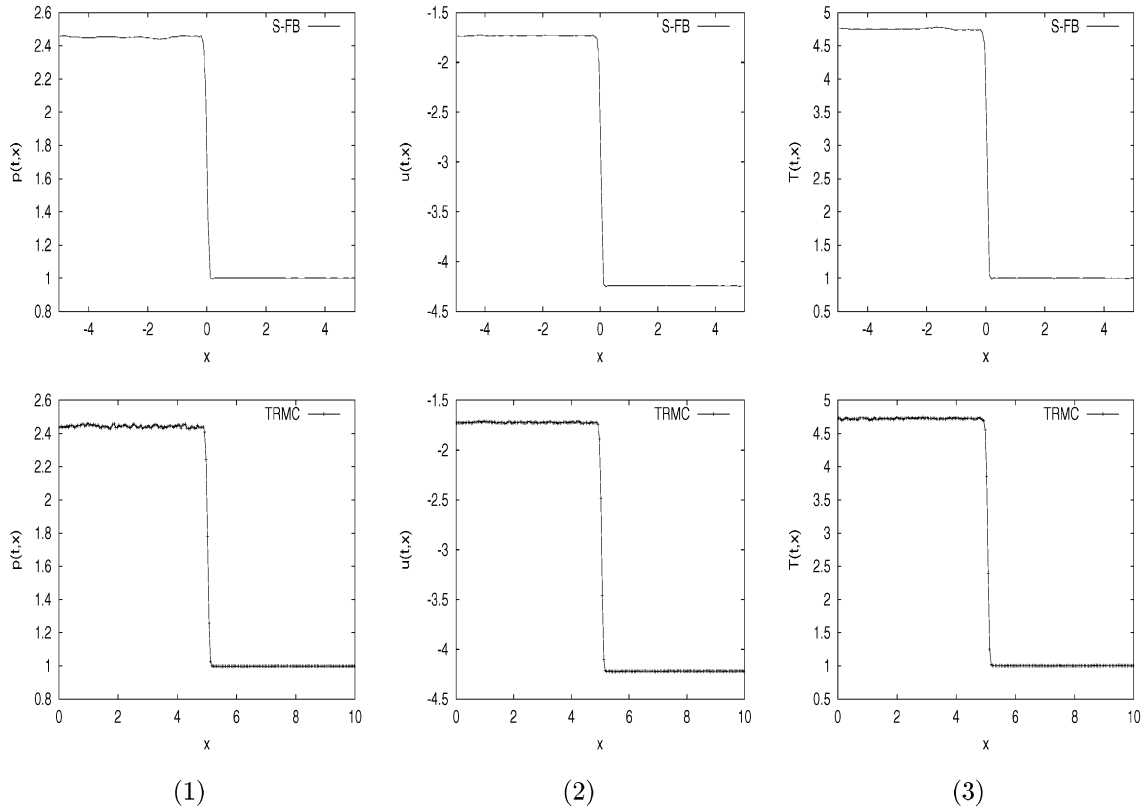
Fig. 6. Shock profiles ($\epsilon = 10^{-2}$): (1) the density ρ, (2) mean velocity u and (3) temperature T obtained by the S-PFC method (up) and by the TRMC method (bottom).

for the time independent BGK operator, but not for the full time dependent Boltzmann equation for hard sphere molecules.

Consider a rarefied gas between two parallel plane walls at $y = 0$ and $y = 1$. Both walls have a common periodic temperature distribution T_w,

$$T_w(x) = 1 - 0.5 \cos(2\pi x) \quad \forall x \in (0, 1),$$

and a common small mean velocity u_w of order Kn in its plane

$$u_w(x) = (Kn, 0).$$

On the basis of kinetic theory, we numerically investigate the behavior of the gas, especially the temperature field, for various small Knudsen numbers Kn. Then, we will assume:

- The behavior of the gas is described by the Boltzmann equation for hard sphere molecules.
- The gas molecules make diffuse reflection on the walls (complete accommodation).
- The solution is 1-periodic with respect to x. Then, the average of pressure gradient in the x-direction is zero.

In this example, the walls are moving with a speed of order Kn. The isothermal lines and the velocity field for $Kn = 0.05$ are shown in Fig. 8. These results are in good agreement with those obtained by discretizing
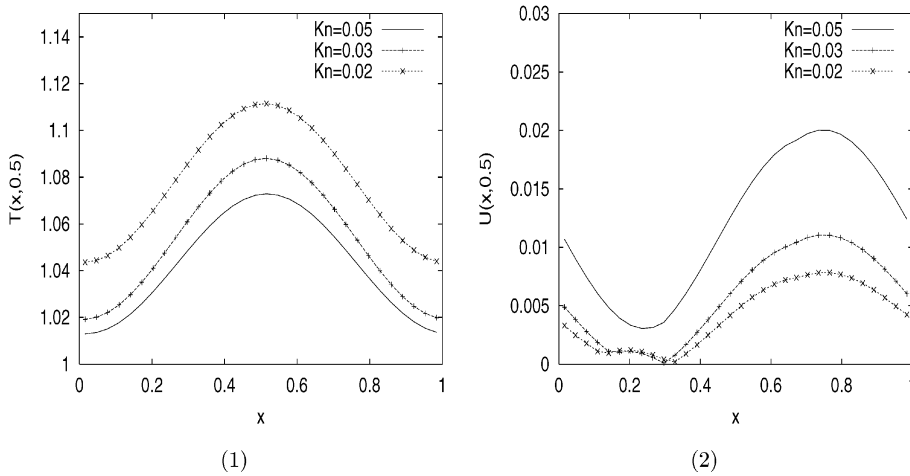
Fig. 7. Ghost effect: temperature and mean velocity along $y = $ const. for various Knudsen numbers $Kn = 0.05, 0.03, 0.02$ (1) temperature at $y = 0.5$ (2) mean velocity u at $y = 0.5$.
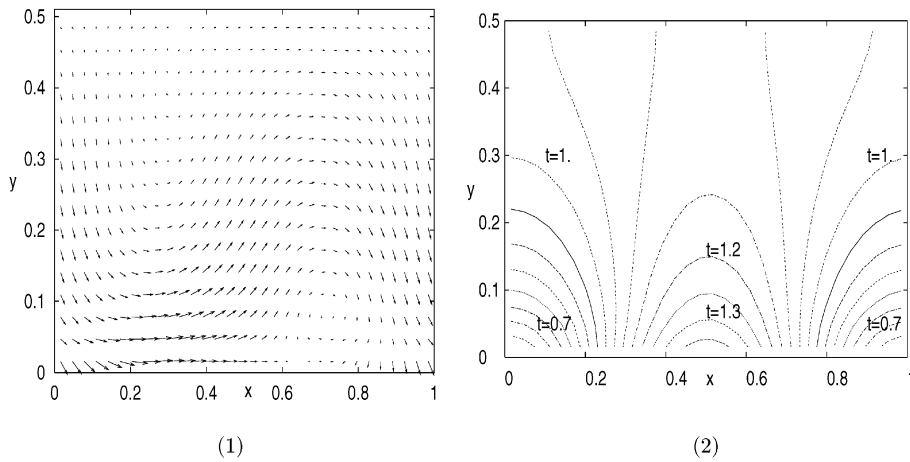

Fig. 8. Ghost effect: (1) velocity field u, (2) isothermal lines for a fixed Knudsen number $Kn = 0.02$.

the the BGK operator [23]. Moreover, according to the numerical simulations presented in [23], the temperature field deviates from one given by the heat conduction equation and is increasing when the Knudsen number Kn goes to zero whereas the velocity flow is vanishing (Fig. 7). In Table 4, we have reported the value of the temperature, solution of the non-homogeneous Boltzmann equation, with respect to the Knudsen number Kn. Then, the temperature converges to the temperature given by the Asymptotic theory developed by Sone et al. [23] and not to the solution of the heat equation. Let us note that in this particular case, we cannot compute an accurate solution for very small Knudsen number, because the computational time to reach the stationary solution with a very good accuracy becomes too large.

We also remark that the agreement has to be interpreted as a qualitative one, since the computations and the analysis performed by Sone et al. concerns the Boltzmann equation with 3D in velocity, while our calculations are performed on the Boltzmann equation with only 2D in velocity.

Table 4
Ghost effect: temperature at $(x, y) = (0, 1/2)$ with respect to the Knudsen number Kn and temperature given by the asymptotic theory (Sone et al.) and by the solution of the heat-conduction equation

	Temperature	Mean velocity
$Kn = 0.05$	1.0129	0.0107
$Kn = 0.03$	1.0228	0.0049
$Kn = 0.02$	1.0436	0.0033
Asymptotic theory	1.045	
Heat-conduction equation	1.018	

The last column corresponds to the mean velocity at $(x, y) = (0, 1/2)$.

5. Conclusions

In this paper we present an accurate deterministic method for the numerical approximation of the space non-homogeneous, time dependent Boltzmann equation. The method, based on a fractional step approach, couples a positive and flux conservative scheme for the treatment of the transport step with a Fourier spectral method for the collision step.

It possesses a high order of accuracy for this kind of problems. In fact it is second order accurate in time, third order accurate in space, and spectrally accurate in velocity. The high accuracy is evident from the quality of the numerical results that can be obtained with a relatively small number of grid points in velocity domain.

An effective time discretization allows the treatment of problems with a considerable range of mean free path, and the decoupling between the transport and the collision step makes it possible the use of parallel algorithms, which become competitive with state-of-the-art numerical methods for the Boltzmann equation.

The numerical results, and the comparison with other techniques, show the effectiveness of the present method for a wide class of problems. There are, however, some limitations of the method in its present form, and several improvements are possible in different directions.

The first limitation is that, because of the $O(n^2)$ complexity, the method is presently very expensive for realistic Boltzmann equation with 3D in velocity. Some research is needed in order to reduce the complexity in the computation of the collision operator in Fourier space. As a first step in this direction, a fast, low storage technique can be used for the table look up of the Fourier coefficient of the collisional operator [12]. We plan to use this storage algorithm and fast, parallel machines for space non-homogeneous 3D calculations with 32^3 modes per cell.

Another drawback of the method is that, in the present form, it is not able to deal with distribution functions that are not well approximated by a periodic function with a reasonable number of Fourier modes. For the above reason, the method can be successfully used only for systems not very far from local equilibrium.

A second serious problem arises with space non-homogeneous problems, and concerns the use of an optimal grid in velocity space. In the present paper we assume that the grid in velocity space is the same for each space cell of the computational domain.

This is certainly a serious limitation if large variations in the mean velocity and/or in the temperature are present in the flow, since a grid that is suitable in a given cell might be inadequate in a different space cell.

Two possible strategies are under consideration to overcome this problem. One is based on a variable grid method, in which different points in space have a different grid in velocity. The passage from one grid to another is performed by weighting and interpolation, as is done in multigrid methods.

A second strategy consists in scaling the velocity variable as

$$v = u + \sqrt{2T}\xi.$$

The function f will be expressed as $f(t,x,v) = f(t,x,u + \sqrt{2T}\xi) = \tilde{f}(t,x,\xi)$. The evolution equation for $\tilde{f}$ will be coupled with the evolution equations for u and T. Such approach, although very attractive, presents several numerical difficulties, and is presently under investigation.

Acknowledgements

References

[1] H. Babovsky, On a simulation scheme for the Boltzmann equation, Math. Methods Appl. Sci. 8 (1986) 223–233.

[2] G.A. Bird, Molecular gas dynamics, Clarendon Press, Oxford, 1994.

[3] A.V. Bobylev, S. Rjasanow, Difference scheme for the Boltzmann equation based on the fast Fourier transform, Eur. J. Mech. B/Fluids 16 (1997) 293–306.

[4] C. Buet, A discrete velocity scheme for the Boltzmann operator of rarefied gas dynamics, Transport Theory Statist. Phys. 25 (1996) 33–60.

[5] C. Cercignani, The Boltzmann equation and its applications, Springer, Berlin, 1988.

[6] C. Cercignani, R. Illner, M. Pulvirenti, The mathematical theory of dilute gases, Springer, New York, 1995.

[7] O. Coulaud, E. Sonnendrücker, E. Dillon, P. Bertrand, A. Ghizzo, Parallelization of semi-Lagrangian Vlasov Codes, J. Plasma Phys. 61 (1999) 435–448.

[8] E. Fijalkow, A numerical solution to the Vlasov equation, Comput. Phys. Commun. 116 (1999) 319–328.

[9] F. Filbet, E. Sonnendrücker, P. Bertrand, Conservative numerical schemes for the Vlasov equation, J. Comput. Phys. 172 (2001) 166–187.

[10] D. Goldstein, B. Sturtevant, J.E. Broadwell, Investigation of the motion of discrete velocity gases, Rar. Gas. Dynam., Progr. Astronautics e Aeronautics, 118, AIAA, Washington, 1989.

[11] T. Inamuro, B. Sturtevant, Numerical study of discrete velocity gases, Phys. Fluids A 12 (1990) 2196–2203.

[12] R. Kirsch, private communication.

[13] K. Nanbu, Direct simulation scheme derived from the Boltzmann equation. I. Monocomponent gases, J. Phys. Soc. Jpn. 52 (1983) 2042–2049.

[14] H. Nessyahu, E. Tadmor, Nonoscillatory central differencing for hyperbolic conservation laws, J. Comput. Phys. 87 (1990) 408–463.

[15] T. Ohwada, Higher order approximation methods for the Boltzmann equation, J. Comput. Phys. 139 (1998) 1–14.

[16] L. Pareschi, B. Perthame, A Fourier spectral method for homogeneous Boltzmann equations, Transport Theory Statist. Phys. 25 (1996) 369–383.

[17] L. Pareschi, G. Russo, On the stability of spectral methods for the homogeneous Boltzmann equation, in: Proceedings of the Fifth International Workshop on Mathematical Aspects of Fluid and Plasma Dynamics (Maui, HI, 1998), Transport Theory Statist. Phys. 29 (2000) 431–447.

[18] L. Pareschi, G. Russo, Numerical solution of the Boltzmann equation. I. Spectrally accurate approximation of the collision operator, SIAM J. Numer. Anal. 37 (2000) 1217–1245.

[19] L. Pareschi, G. Russo, Time Relaxed Monte Carlo methods for the Boltzmann equation, SIAM J. Sci. Comput. 23 (2001) 1253–1273.

[20] F. Rogier, J. Schneider, A direct method for solving the Boltzmann equation, Transport Theory Statist. Phys. 23 (1994) 313–338.

[21] C.-W. Shu, Essentially non-oscillatory and weighted essentially non-oscillatory schemes for hyperbolic conservation laws, in: B. Cockburn, C. Johnson, C.-W. Shu, E. Tadmor (Eds.), Advanced Numerical Approximation of Nonlinear Hyperbolic Equations, in: A. Quarteroni (Ed.), Lecture Notes in Mathematics, 1697, Springer, Berlin, 1998, pp. 325–432.

[22] J.A. Carrillo, I.M. Gamba, A. Majorana, C.-W. Shu, A WENO-solver for the transients of Boltzmann–Poisson system for semiconductor devices, A Performance and comparisons with Monte Carlo methods, J. Comput. Phys. 184 (2003) 498–525.

[23] Y. Sone, K. Aoki, S. Takata, H. Sugimoto, A.V. Bobylev, Inappropriateness of the heat-conduction equation for description of a temperature field of a stationary gas in the continuum limit: examination by asymptotic analysis and numerical computation of the Boltzmann equation, Phys. Fluids 8 (1996) 628–638.

[24] G. Strang, On the construction and comparison of difference schemes, SIAM J. Numer. Anal. 5 (1968) 506–517.
[25] G.B. Whitham, Linear and nonlinear waves, Wiley/Interscience, New York, 1974.
[26] E. Wild, On Boltzmann's equation in the kinetic theory of gases, Proc. Cambridge Philos. Soc. 47 (1951) 602–609.